Scientia Iranica C (2011) 18 (6), 1332–1342

Sharif University of Technology

Scientia Iranica

Transactions C: Chemistry and Chemical Engineering

www.sciencedirect.com

Theoretical, NMR study, kinetics and a mechanistic investigation of the reaction between triphenylphosphine, dialkyl acetylenedicarboxylates and acetyl acetone

S.M. Habibi-Khorassani [a,*], A. Ebrahimi [a], M.T. Maghsoodlou [a], Z. Khajehali [a], M. Zakarianezhad [b]

[a] *Department of Chemistry, University of Sistan and Baluchestan, Zahedan, P.O. Box 98135-674, Iran*

[b] *Department of Chemistry, Faculty of Science, Payam Noor University, Sirjan Center, Sirjan, Iran*

Received 26 October 2010; revised 21 January 2011; accepted 1 May 2011

KEYWORDS

Stable phosphorus ylides;
Dialkyl acetylenedicarboxylates;
Z- and E- isomers;
AIM method;
Acetyl acetone.

Abstract In the present work, a quantum mechanical calculation was clarified as to how the ylides exist in solution as a mixture of two geometrical isomers (Z- and E-) in a major or minor form. In addition, kinetic studies were undertaken for the reaction between triphenylphosphine, di-tert-butyl acetylenedicarboxylate in the presence of a protic/nucleophilic reagent, such as acetyl acetone. To determine the kinetic parameters of the reaction, it was monitored by UV spectrometry. The values of the second order rate constant (k_2) were calculated using standard equations within the program. At the temperature range studied, the dependence of the second order rate constant (Ln k_2) on the reciprocal temperature was in a good agreement with the Arrhenius equation. This provided relevant plots for calculating the activation energy of the reaction. Furthermore, useful information was obtained from studies of the effect of solvents, the structure of reactants (different alkyl groups within the dialkyl acetylenedicarboxylate) and also the concentration of reactants on the rate of reaction. The proposed mechanism was confirmed according to the obtained results and steady state approximation. The first and third (k_3) steps of the reaction were recognized as the determining rates and fast steps, respectively, on the basis of experimental data.

1. Introduction

The reaction of triphenylphosphine with dialkyl acetylenedicarboxylates in the presence of strong CH-acids, such as acetylacetone, methylacetoacetate, cyclopentane-1, 3-dione or 5, 5-dimethylcyclohexane-1, 3-dione(dimedone), has been studied. In some cases, stable phosphorus ylides are obtained in excellent ylides. The ylide moiety of these compounds is strongly conjugated with the adjacent carbonyl group, and rotation around the partial double bond in (E-) and (Z-) geometrical isomers is slow on the NMR time scale at ambient temperature. Thus, these ylides exist as a mixture of geometrical isomers. From the reaction of dimedone with dimethyl acetylenedicarboxylate (DMAD) in the presence of triphenylphosphine, a chromene derivative is obtained. There are many studies on the reaction between trivalent phosphorus nucleophiles and acetylenic esters in the presence of OH, NH or CH acides [1–9]. In some cases, ylide products are stable, but in other cases they cannot be isolated and appear to accrue as an intermediate on the pathway to an observed product. In continuation of our current interest in the development of new approaches to heterocyclic and carbocyclic systems, kinetics and mechanistic studies, along with theoretical calculations of a facile synthesis of the reaction between triphenylphosphine 1, dialkyl acetylenedicarboxylates 2 and acetyl acetone 3 (as a protic/nucleophilic reagent), were investigated for generation of phosphorus ylides 4a–c, involving two geometrical isomers,

* Corresponding author.
E-mail address: smhabibi_usb@yahoo.com (S.M. Habibi-Khorassani).

1026-3098 © 2012 Sharif University of Technology. Production and hosting by Elsevier B.V. All rights reserved. Peer review under responsibility of Sharif University of Technology.

doi:10.1016/j.scient.2011.08.011

Production and hosting by Elsevier

such as Z- and E- isomersm, synthesis of which was reported earlier [10]. For assignment of the two Z- and E- isomers in a minor or major form in phosphorus ylides 4a–b containing acetyl acetone, first the Z- and E- isomers were optimized for all ylide structures at the HF/6-31G(d,p) level of theory by the Gaussian 03 package program. The relative stabilization energies of both geometrical isomers have been calculated at the B3LYP/6-311++G** level. Atoms In Molecules (AIM) and Natural Population Analysis (NPA) methods, and the CHelpG keyword at the HF/6-31G(d,p) level of theory have been performed in order to gain a better understanding of the most geometrical parameters of both E-4(a,b) and Z-4(a,b) of phosphorus ylides. The numbers of critical points and intramolecular hydrogen bonds, as well as the charge of atoms that constructed on the Z- and E- isomers, have been recognized. The results altogether reveal the effective factors on the stability of Z- and E- ylide isomers. In addition, J_{x-y}, the values of proton and carbon coupling constants, and also chemical shifts (δ^{H}_{iso}, δ^{C}_{iso}) have been calculated at a mentioned level, using the SPINSPIN keyword.

2. Material and methods

Quantum mechanical calculation has been performed using the Gaussian 03 and AIM2000 program packages. Dialkyl acetylenedicarboxilate, triphenylphosphine and acetyl acetone were purchased from Fulka (Buchs, Switzerland) and used without further purification. All extra pure solvents, including 1, 2-dichloroethane and 1, 4-dioxane, were also obtained from Merk (Darmstadt, Germany). A Cary UV/Vis spectrometer model Bio-300 with a 10 mm light-path black quartz spectrophotometer cell was employed throughout the current work.

3. Results and discussion

3.1. Theoretical study

Recently, different reports have been published on the synthesis of stable phosphorus ylides from the reaction between triphenylphosphine and reactive acetylenic esters in the presence of N–H, C–H or S–H heterocyclic compounds. These ylides usually exist as a mixture of the two geometrical isomers, although some ylides exhibit one geometrical isomer. Assignment of the stability of the two Z- and E-isomers is impossible in phosphorus ylides by experimental methods, such as ^{1}H and ^{13}CNMR and IR spectroscopies, mass spectrometry and elemental analysis data. For this reason, quantum mechanical calculation has been performed in order to gain a better understanding of the most important geometrical parameters and also the relative energies of both geometrical isomers.

4. Calculations

4.1. Structure and stabilities

In order to determine a more stable form of both geometrical isomers [Z-4(a,b) and E-4(a,b)] of ylides (4a or 4b), which is shown in Figure 1, first their structures were optimized at the HF/6-31G(d,p) level of theory [11] using the Gaussian 03 package program [12]. Also, the relative stabilization energy of the two isomers has been calculated at HF/6-31G(d,p) and B3LYP/6-311++G** levels (see Figures 2 and 3). The relative stabilization energies for the two [Z-4(a,b) and E-4(a,b)] isomers are reported in Table 1. As seen, E-4a and E-4b isomers are more stable than Z-4a and Z-4b forms (0.53 and 0.22 kcal/mol, respectively) at the B3LYP level.

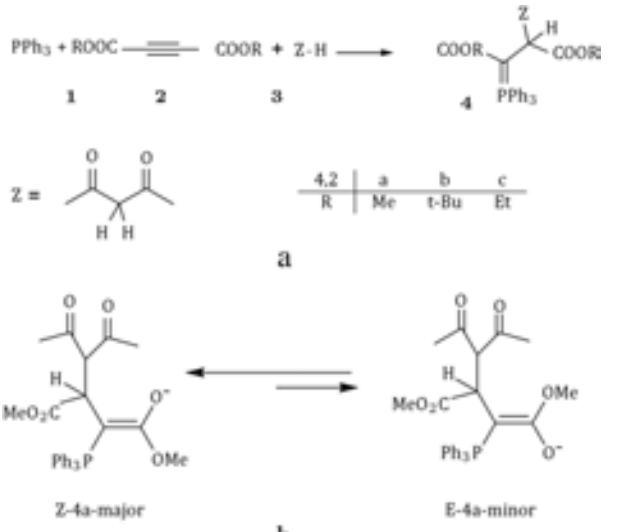

Figure 1: (a) The reaction between triphenylphosphine 1, dialkyl acetylenedicarboxylate 2 (2a or 2b) and acetyl acetone 3 for generation of stable phosphorus ylides 4 (4a or 4b). (b) The two isomers E-4a and Z-4a (major and minor, respectively) of ylide 4a.

Table 1: The relative energy (kcal/mol) for both the Z- and E-isomers of ylides 4a and 4b, obtained at HF/6-31G (d,p) and B3LYP/6-311++G(d,p) levels.

Geometrical isomer	HF	B3LYP
Z-4a	0.59	0.53
E-4a	0.00	0.00
Z-4b	0.26	0.22
E-4b	0.00	0.00

Further investigation was undertaken in order to determine more effective factors regarding the stability of the two Z- and E-isomers, on the basis of AIM calculations [13], at the HF/6-31G(d,p) level of theory, by the AIM2000 program package [14]. In recent years, the AIM theory has often been applied to the analysis of H-bonds. In this theory, the topological properties of the electron density distribution are derived from the gradient vector field of the electron density, $\nabla\rho(r)$, and on the Laplacian of the electron density, $\nabla^2\rho(r)$.

The Laplacian of the electron density, $\nabla^2\rho(r)$, identifies regions of space wherein the electronic charge is locally depleted [$\nabla^2\rho(r) > 0$] or built up [$\nabla^2\rho(r) < 0$] [13]. Two interacting atoms in a molecule form a critical point in the electron density, where $\nabla\rho(r) = 0$, called the Bond Critical Point (BCP). The values of the charge density and its Laplacian at these critical points give useful information regarding the strength of the H-bonds [14]. The ranges of $\rho(r)$ and $\nabla^2\rho(r)$ are 0.002–0.035 e/a_0^3 and 0.024–0.139 e/a_0^5, respectively, if H-bonds exist [15]. The AIM calculation indicates intramolecular Hydrogen-Bond Critical Points (H-BCP) for the two Z-4(a,b) and E-4(a,b) isomers. Intramolecular H-BCPs along with a part of the molecular graphs for the two rotational isomers are shown in Figures 2 and 3 (dotted line). Most important geometrical parameters involving some H-bonds (bond length and their relevant bond angle) are reported in Table 2. The electron density (ρ) $\times$ 10^3, Laplacian of electron density, $\nabla^2\rho(r)$ $\times$ 10^3, and energy density, $-H(r)$ $\times$ 10^4, are also

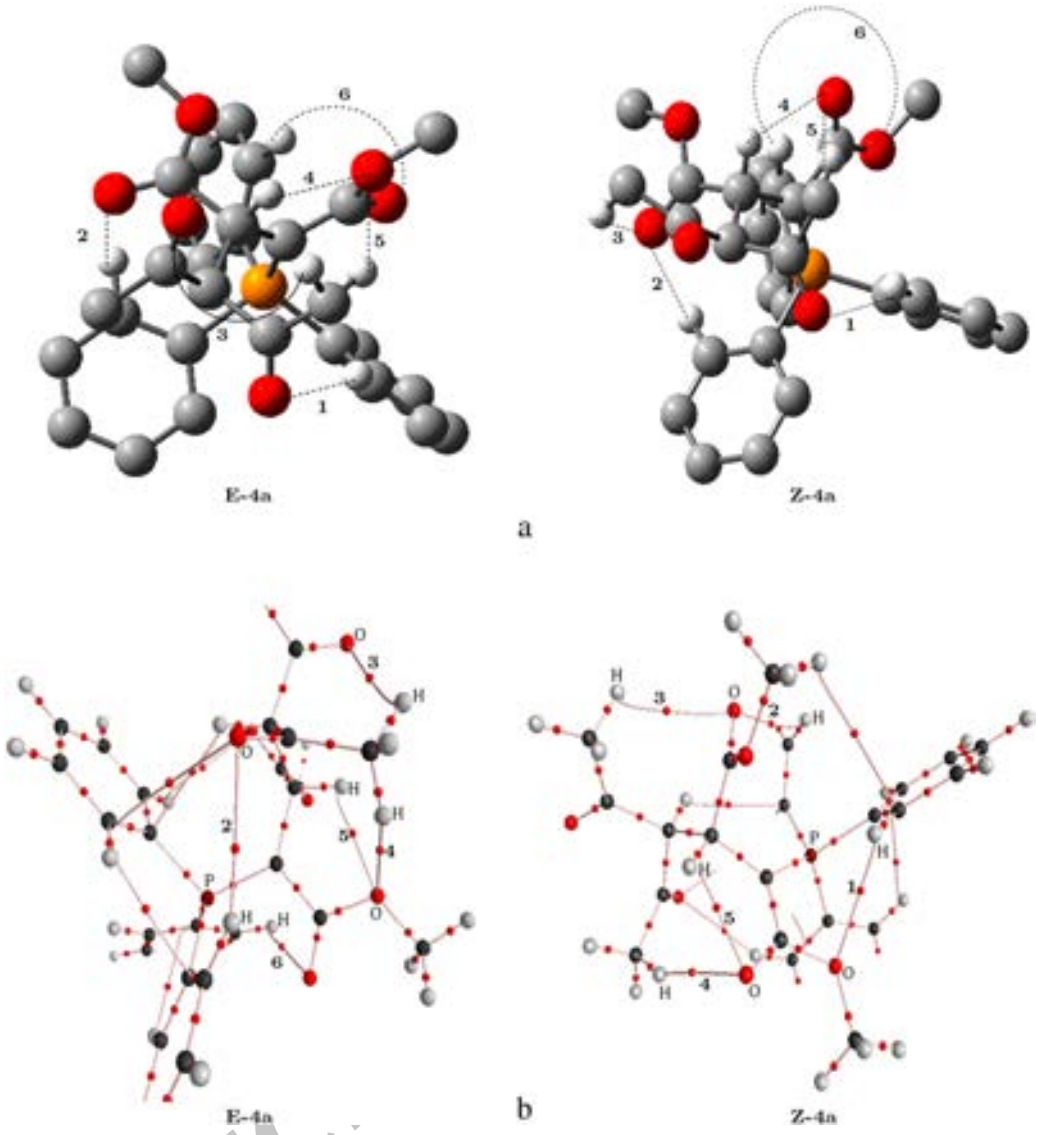

Figure 2: (a) Intermolecular hydrogen bonds (dotted lines) in the two E-4a and Z-4a geometrical isomers of stable ylide 4a. (b) A part of molecular graphs, including intermolecular hydrogen Bond Critical Points (BCPS) for the two rotational isomers such as E-4a and Z-4a. Small red spheres and lines correspond to BCPS bond paths, respectively.

reported in Table 3. A negative total energy density at the BCP reflects a dominance of potential energy density, which is the consequence of accumulated stabilizing electronic charge [16]. Herein, the number of hydrogen bonds in both categories (E-4a and Z-4a) and (E-4b and Z-4b) are (5 and 5) and also (9 and 9), respectively. The values of ρ and $\nabla^2\rho(r)$ for those are in the ranges (0.008–0.018 and 0.007–0.019 e/a_0^3) and (0.008–0.018 and 0.008–0.019 e/a_0^3), and also (0.019–0.075 and 0.029–0.082 e/a_0^5) and (0.023–0.076 and 0.026–0.081 e/a_0^5), respectively. In addition, the Hamiltonian $[-H(r) \times 10^4]$ are in the ranges (6.81–17.70 and 4.22–19.94 au) and (7.14–15.96 and 3.95–19.88 au), respectively (see Table 3). These HBs show $\nabla^2\rho(r) > 0$ and $H(r) < 0$, which, according to the classification of Rozas et al. [17], are medium-strength hydrogen bonds. In both ylides (see Table 4), the dipole moment for the two E-4a and E-4b isomers (4.79 and 4.59 D) are smaller than the two Z-4a and Z-4b isomers (7.97 and 7.88 D, respectively), and the value of $-H_{tot}\left(=\sum -H(r) \times 10^4\right)$ for the two E-4a and E-4b isomers (69.97 and 104.65 au) are smaller than the two Z-4a and Z-4b isomers (73.26 and 108.81 au, respectively). Although dipole moments in both the Z-4(a,b) are more than the E-4(a,b) and appear as an effective factor on the instability of the Z-4(a,b), the values of $-H_{tot}$ in the Z-4(a,b), which are larger than E-4(a,b), are an important fact regarding the stability of Z-4(a,b). It seems that stability on both E-4(a,b) stems from two opposite factors (dipole moment and total Hamiltonian) in which the influence of the total Hamiltonian is superior to that of the dipole moment. Differences of $-H_{tot}$ between Z-4a and E-4a (3.38 au) and also Z-4b and E-4b (4.16 au), as a stability factor, are larger than differences of dipole moment between Z-4a and E-4a (3.16 D) and also Z-4b and E-4b (3.29 D) as an instability factor. Hence, the effect of $-H(r)$ is dominant on the influence of dipole moment in the Z-4(a,b) category. As a result, Z-4a and Z-4b are slightly stable isomers in comparison with E-4a and E-4b. Although, on the basis of theoretical calculations (Table 1), both E-4a and E-4b have a slightly stability with respect to the two Z-4a and Z-4b (0.53 and 0.22 kcal/mol, respectively) isomers and seems to be different from the results

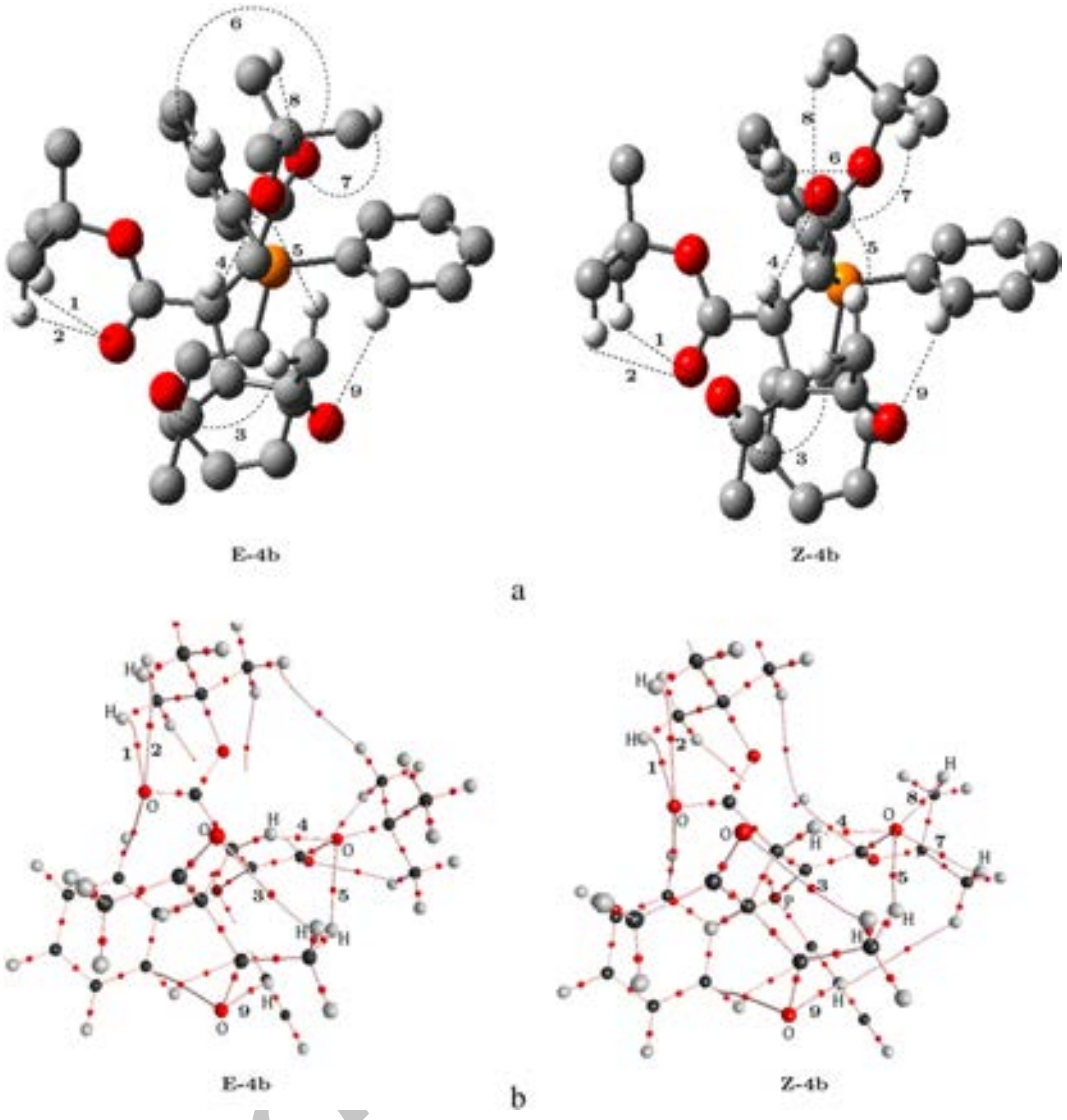

Figure 3: (a) Intermolecular hydrogen bonds (dotted lines) in the two E-4b and Z-4b geometrical isomers of stable ylide 4b. (b) A part of molecular graphs, including intermolecular hydrogen Bond Critical Points (BCPS) for the two rotational isomers such as E-4b and Z-4b. Small red spheres and lines correspond to BCPS bond paths, respectively.

of predictable properties of the most important geometrical parameters (Table 4). Perhaps, this slightly different behavior is relevant to the huge structures of the two ylides 4(a,b) involving three large atoms such as the six oxygen atoms and phosphorus and the large number of other atoms (C and H). This point limited the application of a basis set higher than HF/6-31G(d,p), at a higher performance, to gain more accurate calculations. Nevertheless, the results involving the large difference of $-H_{tot}$ as a dominate factor of stability over the small difference of the dipole moment as an instability factor in the Z- 4(a,b) category are compatible with the experimental results of the ^{1}H, ^{13}C, ^{31}P NMR spectroscopes which indicate the two isomers of Z-4a and Z-4b, with the experimental abundance percentage of 60 and 65 (major forms), with respect to the E-4(a,b) (minor forms).

Also, the charge on different atoms, which are calculated by Atoms In Molecules (AIM) and Natural Population Analysis (NPA) methods, and also the CHelpG keyword at the HF/6-31G(d,p) level are reported in Table 5 for the two Z- and E-isomers of ylides 4a and 4b. There is good agreement between the results of these three methods.

Table 2: Most important rotational parameters corresponding to H-bonds (bond lengths and their relevant angles) for the two Z- and E-isomers in both ylides 4a and 4b. Bond lengths in Angstroms and bond angles in degrees, respectively.

E-4a			Z-4a
$C_{32}H_{35}\cdots O_5$	2.72[a] (106.03)[b]	$C_{32}H_{35}\cdots O_5$	2.50[a] (107.33)[b]
$C_{22}H_{26}\cdots O_{42}$	2.52 (117.56)	$C_{22}H_{26}\cdots O_{43}$	2.64 (112.80)
$C_{60}H_{63}\cdots O_{43}$	2.55 (148.06)	$C_{60}H_{62}\cdots O_{42}$	2.45 (157.67)
E-4b			Z-4b
$C_{61}H_{69}\cdots O_5$	2.48[a] (110.43)[b]	$C_{74}H_{82}\cdots O_5$	2.48[a] (110.42)[b]
$C_{22}H_{26}\cdots O_{42}$	2.45 (118.78)	$C_{52}H_{55}\cdots O_{42}$	2.43 (155.07)
$C_{52}H_{55}\cdots O_{43}$	2.56 (147.48)	$C_{22}H_{26}\cdots O_{43}$	2.58 (114.75)

[a] Bond length.
[b] Bond angle.

The individual chemical shifts have been characterized by NMR calculations at the mentioned level using the SPINSPIN

Table 3: The values of $a = \rho \times 10^3$, $b = \nabla^2\rho \times 10^3$ and $c = -\mathrm{H}(r) \times 10^4$ for both the Z-4(a,b) and E-4a isomers of ylide 4a and 4b calculated at the hydrogen bond critical points. All quantities are in atomic units.

E	a	b	c	Z	a	b	c
1	6.22[a] (5.19)[b]	23.16[a] (19.92)[b]	8.94[a] (9.02)[b]	1	7.12[a] (8.27)[b]	26.2[a] (29.56)[b]	8.56[a] (7.49)[b]
2	11.54 (7.28)	45.2 (27.88)	13.42 (11.60)	2	11.54 (10.51)	45.28 (41.68)	13.58 (14.66)
3	8.78 (8.62)	33.84 (33.36)	11.89 (11.99)	3	8.84 (9.42)	34.24 (36.44)	12.64 (14.37)
4	18.39 (17.95)	76.08 (75.84)	15.96 (17.70)	4	19.22 (19.19)	81.96 (82.36)	19.88 (19.94)
5	8.14 (8.23)	29.56 (29.64)	7.14 (6.81)	5	10.46 (10.12)	34.68 (33.68)	3.95 (4.22)
6	11.20 (9.77)	43.84 (39.40)	11.99 (12.85)	6	8.81 (7.85)	36.16 (32.80)	12.76 (12.58)
7	13.01	49.28	11.78	7	13.04	49.96	12.76
8	13.27	50.72	12.65	8	13.53	51.28	12.00
9	12.31	47.52	12.88	9	12.19	46.96	12.68

[a] Are relevant to the two E-4a and Z-4a isomers, respectively.
[b] Are relevant to the two E-4b and Z-4b isomers, respectively.

Table 4: The most important geometrical parameters involving the value of H_{tot}/au, dipole moment/D and the number of hydrogen bonds for the two Z- and E-isomers of ylides 4a and 4b.

Geometrical isomer	H_{tot}/au	Dipole moment/D	Number of Hydrogen bond
E-4a	69.97	4.79	5
Z-4a	73.26	7.97	5
E-4b	104.65	4.59	9
Z-4b	108.81	7.88	9

keyword. The total spin–spin coupling constant is the sum of four components: the Paramagnetic Spin-Orbit (PSO), Diamagnetic Spin-Orbit (DSO), Fermi-Contact (FC) and Spin-Dipole (SD) terms. The values of chemical shifts (δ) and coupling constants (J_{x-y}) are reported in Tables 6–9 for the two minor E-4(a,b) and major Z-4(a,b) geometrical isomers. As seen, there is good agreement between both the experimental [10] and theoretical chemical shifts (δ) and coupling constants (J_{x-y}). In the present work, molecular structures of ylides 4a–b, involving large atoms, such as six oxygen atoms and one phosphorus atom, are huge along with the large numbers of other atoms. For this reason, employment of a higher level of theory, with the basis set higher than HF/6-31G(d,p), is impossible for a higher performance to gain more accurate calculations.

Table 6: Selected ^{1}H NMR chemical shift (δ in ppm) for some functional groups in the E-4a isomer as a minor form.

Groups	δ^H/ppm
6H, 2s, $2CH_3$	2.10–2.22[a] (1.80–2.35)[b]
6H, 2s, $2OCH_3$	3.00–3.54 (3.08–3.50)
1H, d, P–C=CH	3.46 (2.06)
15H, m, $3C_6H_5$	7.41–7.57 (7.40–7.60)

[a] Experimental data in accord with the results reported in the literature.
[b] Theoretical data.

Table 7: Selected ^{1}H NMR chemical shift (δ in ppm) for some functional groups in the Z-4a isomer as a minor form.

Groups	δ^H/ppm
6H, 2s, $2CH_3$	2.03–2.14[a] (2.06–2.82)[b]
6H, 2s, $2OCH_3$	3.54 (3.55)
1H, d, P–C=CH	2.90 (2.11)
15H, m, $3C_6H_5$	7.41–7.57 (7.43–7.62)

[a] Experimental data in accord with the results reported in the literature.
[b] Theoretical data.

This limitation causes a small difference between both experimental and theoretical coupling constants in some functional groups.

Table 5: The charges on different atoms for the two Z- and E- isomers in both ylides 4a and 4b calculated by AIM, NBORead and CHelpG methods, respectively at HF/6-31G(d,p) theoretical level.

Number of atom	E-4a	Z-4a	E-4b	Z-4b
C1	0.36[a]	0.34	0.37	0.37
	−0.19[b]	−0.19	−0.18	−0.18
	−0.19[c]	−0.19	−0.18	−0.18
C6	-8.53×10^{-1}	-8.80×10^{-1}	-8.03×10^{-1}	-8.09×10^{-1}
	−0.61	−0.64	−0.61	−0.61
	−0.61	−0.64	−0.61	−0.61
C7	1.85	1.86	1.85	1.86
	0.88	0.88	0.91	0.90
	0.88	0.88	0.91	0.90
O42	−1.42	−1.39	−1.43	−1.40
	−0.67	−0.66	−0.69	−0.67
	−0.67	−0.66	−0.69	−0.67
O43	−1.28	−1.30	−1.29	−1.28
	−0.66	−0.67	−0.71	−0.73
	−0.66	−0.67	−0.71	−0.73
P8	3.22	3.21	3.22	3.22
	1.23	1.26	1.23	1.24
	1.23	1.26	1.23	1.24

[a] Calculated by AIM method.
[b] Calculated by NBORead method.
[c] Calculated by CHelpG method.

Table 8: Selected ^{13}C NMR chemical shift (δ in ppm) and coupling constants (J in Hz) for some functional groups in the E-4a isomer as a minor form.

Groups	δ^C/ppm	J_{PC}/Hz
2 CH_3	26.72–28.99[a] (24.00–28.70)[b]	
d, P–C	35.61 (31.63)	
d, P–C=CH	40.58 (37.85)	
2 OMe	45.04–47.98 (46.38–46.90)	
CH	63.07 (61.73)	
d, C_{ipso}	123.24 (124.94)	89 (88)
d, C_{meta}	124.72 (124.57)	12 (11.75)
d, C_{para}	128.27 (131.80)	7 (7.91)
d, C_{ortho}	130.17 (133.36)	
P–C=C	165.84 (167.20)	
d, C=O	171.35 (172.21)	
2 C=O	198.22–200.01 (199.45–201.03)	

[a] Experimental data in accord with the results reported in the literature.
[b] Theoretical data.

Table 9: Selected ^{13}C NMR chemical shift (δ in ppm) and coupling constants (J in Hz) for some functional groups in the Z-4a isomer as a minor form.

Groups	δ^C/ppm	J_{PC}/Hz
2 CH_3	26.09–26.72[a] (25.20–26.99)[b]	
d, P–C	35.24 (30.36)	
d, P–C=CH	39.42 (36.10)	
2 OMe	46.37–47.98 (45.53–46.95)	
CH	64.35 (58.70)	
d, C_{ipso}	122.66 (121.05)	83 (87)
d, C_{meta}	124.87 (124.34)	11 (11.30)
d, C_{para}	128.27 (131.58)	7 (7.79)
d, C_{ortho}	130.17 (131.68)	
P–C=C	167.00 (165.70)	
d, C=O	171.35 (172.35)	
2 C=O	198.22–200.16 (200.53–201.28)	

[a] Experimental data in accord with the results reported in the literature.
[b] Theoretical data.

5. Kinetics studies

To gain further insight into the mechanism of the reaction between triphenylphosphin 1, dialkyl acetylene dicarboxylates 2 and acetyl acetone 3 (as a protic/nucleophilic reagent) for generation of phosphorus ylids 4a–b, a kinetics study of the reactions was undertaken using a UV spectrometric technique. The synthesis of these reactions has been reported earlier [10]. First, it was necessary to find the appropriate wavelength to follow the kinetic study of the reaction. For this purpose, in the first experiment, a 3×10^{-3} mol L^{-1} solution of compounds, 1, 2b and 3, was prepared in 1, 4-dioxane as solvent. An approximately 3 mL aliquot from each reactant was pipetted into a 10 mm light path quartz spectrophotometer cell, and the relevant spectra were recorded over the wavelength range, 200–400 nm. Figures 4–6 show the ultraviolet spectra of compounds 1, 2b and 3, respectively. In a second experiment, 1 mL aliquot from 3×10^{-3} mol L^{-1} solutions of each compound of 1 and 3 was pipetted first into a quartz spectrophotometer cell (as there is no reaction between them). Later, 1 mL aliquot of the 3×10^{-3} mol L^{-1} solutions of reactant 2b was added to the mixture and the reaction was monitored by recording scans of the entire spectra every 12 min over the whole reaction time at ambient temperature. The ultra-violet spectra shown in Figure 7 are typical for generation of ylide 4b. From this, the appropriate wavelength was found to be 300 nm (corresponding mainly to reactant 1). Since at this wavelength, compounds 4b, 2b and 3 have relatively no absorbance value, the opportunity was provided to fully investigate the kinetics of the reaction between triphenylphosphine 1, di-tert-butyl

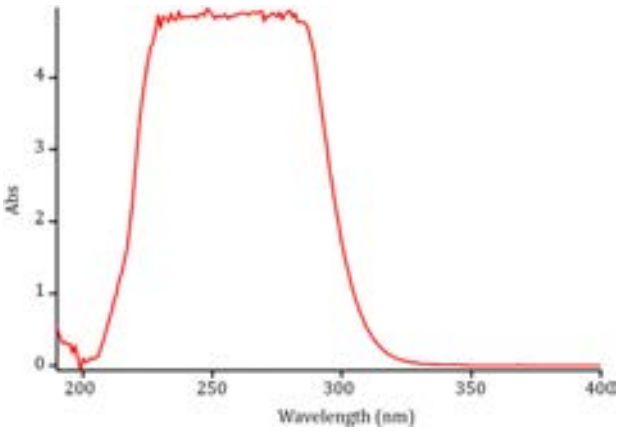

Figure 4: UV spectrum of 10^{-3} mol L^{-1} triphenylphosphine 1 in 1, 4-dioxane.

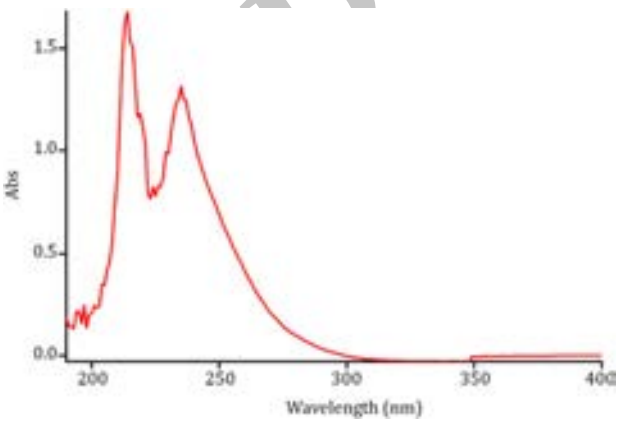

Figure 5: UV spectrum of 10^{-3} mol L^{-1} di-*tert*-butyl-acetylenedicarboxylate 2b in 1, 4-dioxane.

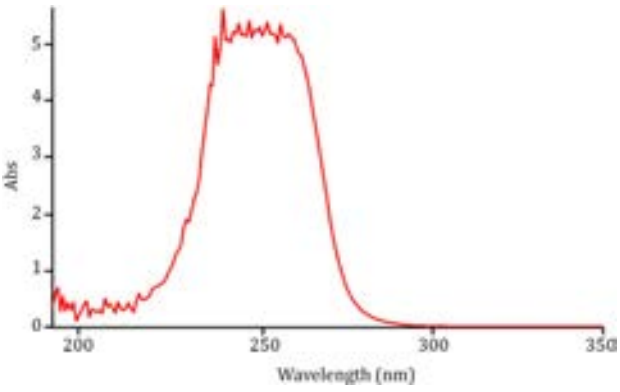

Figure 6: UV spectrum of 10^{-3} mol L^{-1} acetyl acetone 3 in 1, 4-dioxane.

acetylenedicarboxylate 2b and acetyl acetone 3 at 300 nm, in the presence of 1, 4-dioxane as the solvent. Since the spectrophotometer cell of the UV instrument had a 10 mm light-path cuvette, the UV-vis spectra of compound 4b were measured over the concentration range (2×10^{-4} mol $L^{-1} \leq M_{4c} \leq 10^{-3}$ mol L^{-1}) to check for a linear relationship between absorbance values and concentrations. With the suitable concentration range and wavelength identified, the following procedure was employed.

For each kinetic experiment, first a 1 mL aliquot from each freshly made 3×10^{-3} mol L^{-1} solution of compounds 1 and

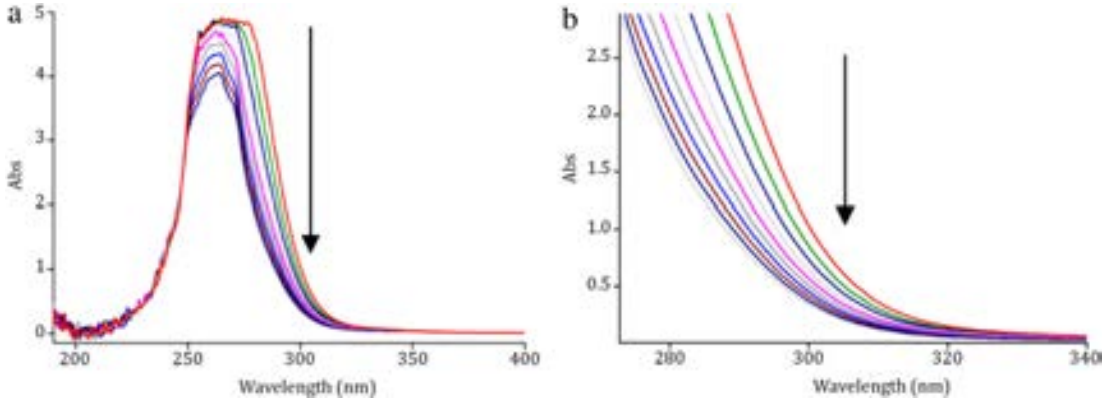

Figure 7: (a) UV spectra of the reaction between 1, 2b and 3 with 10^{-3} mol L^{-1} concentration of each compound proceeds in 1, 4-dioxane with 10 mm light-path cell for generation of ylide 4b. (b) Expanded section of UV spectra over the wavelength range 270–340 nm.

Table 10: Values of overall second order rate constant for the reactions between (1, 2a and 3), (1, 2b and 3) and (1, 2c and 3) in the presence of solvents such as 1, 2-dichloroethane and 1, 4-dioxane, respectively, at all temperatures investigated.

Reactions	Solvent	ε	k_2 mol^{-1} L min^{-1}			
			15.0 °C	20.0 °C	25.0 °C	30.0 °C
1, 2a and 3	1, 4-dioxane	2	518.2	536.2	615.1	692.3
1, 2a and 3	1, 2-dichloroethane	10	599.5	633.1	667.2	800.8
1, 2c and 3	1, 4-dioxane	2	413.6	449.8	501.5	577.9
1, 2c and 3	1, 2-dichloroethane	10	459.1	498.7	572.6	649.9
1, 2b and 3	1, 4-dioxane	2	54.5	64.7	75.6	91.3
1, 2b and 3	1, 2-dichloroethane	10	63.2	78.4	95.1	122.6

3 in 1, 4-dioxane was pipetted into a quartz cell and then a 1 mL aliquot of the 3×10^{-3} mol L^{-1} of the solution of reactant 2b was added to the mixture keeping the temperature at 15.0 °C. The kinetics reaction was followed by plotting the UV absorbance against time. Figure 8 shows the absorbance change (dotted line) versus time for the 1:1:1 addition reaction between compounds 1, 2b and 3 at 15.0 °C. The infinity absorbance (A_∞), i.e. the absorbance at reaction completion, can be obtained from Figure 8 at $t = 103$ min. With respect to this value, zero, the first or second curve fitting could be drawn automatically for the reaction by the software [18] associated with the UV instrument. Using the original experimental absorbance versus time, data provided a second-order fit curve (solid line) that fits exactly the experimental curve (dotted line), as shown in Figure 9. Thus, the reaction between triphenylphosphine 1, di-*tert*-butyl acetylenedicarboxylate 2b and 3 follows second-order kinetics. The second-order rate constant (k_2) is then automatically calculated using a standard equation [18] within the program at 15.0 °C. This is reported in Table 10.

Furthermore, kinetic studies were carried out using the same concentration of each reactant in the continuation of experiments with concentrations of 5×10^{-3} mol L^{-1} and 7×10^{-3} mol L^{-1}, respectively. As expected, the second-order rate constant was independent of concentration and its value was the same as in the previous experiment. In addition, the overall order of the reaction was also 2.

5.1. Effect of solvents and temperature

To determine the effect of changes in temperature and the solvent environment on the rate of reaction, it was elected to perform various experiments under different temperatures and solvent polarities, but otherwise, under the same conditions as for the previous experiment. For this purpose, 1, 2-dichloroethane with a 10 dielectric constant was chosen as a suitable solvent, since it could not dissolve all compounds, neither it react with them. The effects of solvents and temperatures on the rate constant are given in Table 10. The results show that the rate of reaction in each case was increased at higher temperatures. In addition, the rate of reaction between 1, 2b and 3 was accelerated in a higher dielectric constant environment (1, 2-dichloroethane) in comparison with a lower dielectric constant environment (1, 4-dioxane), at all temperatures investigated. In the temperature range studied, the dependence of the second-order rate constant (Ln k_2) of the reactions on reciprocal temperature is consistent with the Arrhenius equation, giving an activation energy of reaction between 1, 2b and 3 (24.7 kJ/mol) from the slope of Figure 10.

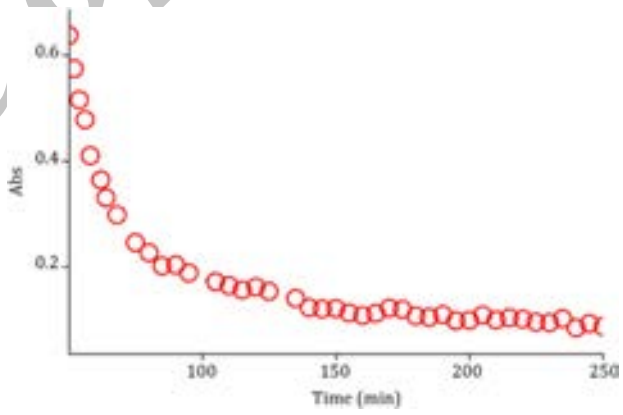

Figure 8: The experimental absorbance changes (dotted line) against time at 300 nm for the reaction between compounds 1, 2b and 3 at 15.0 °C.

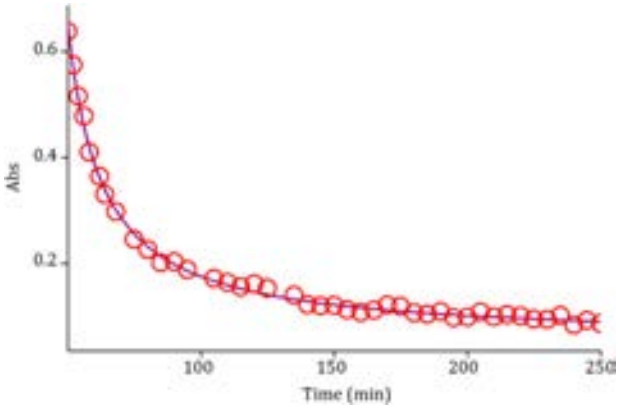

Figure 9: Second order fit curve (solid line) accompanied by the original experimental curve (dotted line) for the reaction between compounds 1, 2b and 3 at 300 nm and 15.0 °C in 1, 4-dioxane.

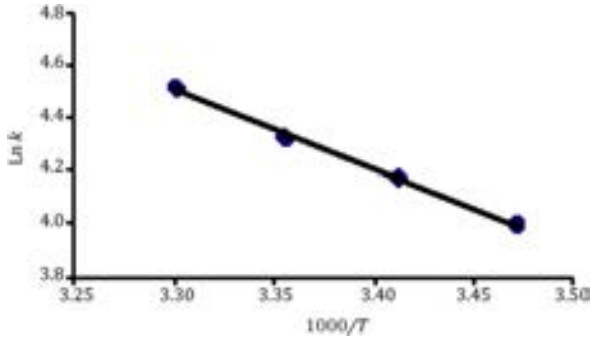

Figure 10: Dependence of second order rate constant (Ln k_2) on reciprocal temperature for the reaction between compounds 1, 2b and 3 measured at wavelength 300 nm in 1, 4-dioxane in accordance with Arrhenius equation.

5.2. Effect of concentration

To determine reaction order, with respect to triphenylphosphine 1 and dialkyl acetylene-dicarboxylate 2 (2b), in continuation of the experiments, all kinetic studies were carried out in the presence of excess 3. Under this condition, the rate equation may therefore be expressed as:

$$\text{rate} = k_{\text{obs}}[1]^{\alpha}[2]^{\beta}, \qquad k_{\text{obs}} = k_2[3]^{\gamma}$$

or:

$$\text{Ln}\, k_{\text{obs}} = \text{Ln}\, k_2 + \gamma \text{Ln}\,[3]. \tag{1}$$

In this case (3×10^{-2} mol L^{-1} of 3 instead of 3×10^{-3} mol L^{-1}), using the original experimental absorbance versus time data provides a second order fit curve (solid line) against time at 335 nm, which exactly fits the experimental curve. The value of the rate constant was the same as that obtained from the previous experiment (3×10^{-3} mol L^{-1}). Repetition of the experiments with 5×10^{-2} mol L^{-1} and 7×10^{-2} mol L^{-1} of 3 gave separately the same fit curve and rate constant. In fact, the experimental data indicated that the observed pseudo second order rate constant (k_{obs}) was equal to the second order rate constant (k_2); this is possible when γ is zero in Eq. (1). It appears therefore that the reaction is zero and second order, with respect to 3 (as a protic/nucleophilic reagent) and the sum of 1 and 2 (2b) ($\alpha + \beta = 2$), respectively.

To determine reaction order, with respect to dialkyl acetylenedicarboxylate 2 (2b), continuation of the experiments was performed in the presence of an excess of 1;

$$\text{rate} = k'_{\text{obs}}[3]^{\gamma}[2]^{\beta}, \quad k'_{\text{obs}} = k_2[1]^{\alpha}. \tag{2}$$

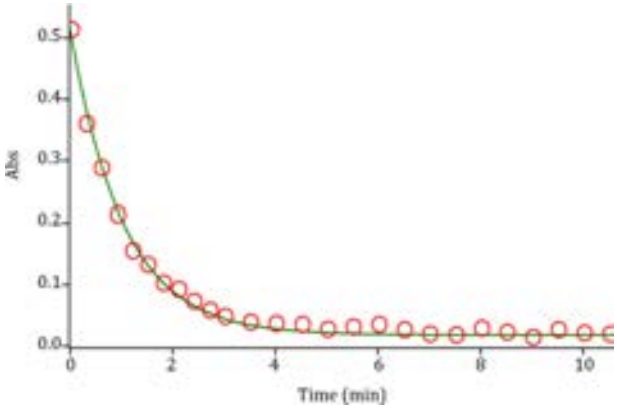

Figure 11: Pseudo first order fit curve (solid line) for the reaction between 1 and 3 in the presence of excess 2 (2b) (10^{-2} mol L^{-1}) at 300 nm and 15.0 °C in 1, 4-dioxane.

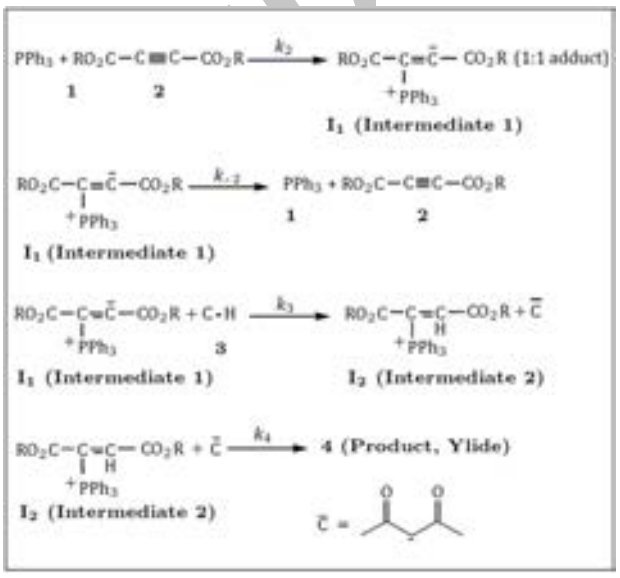

Figure 12: Proposed mechanism for the reaction between 1, 2(2a, 2b or 2c) and 3 on the basis of literature [1–9] for generation of phosphorus ylides 4(4a, 4b or 4c).

The original experimental absorbance versus time data provided a pseudo first order fit curve at 300 nm, which exactly fits the experimental curve (dotted line), as shown in Figure 11.

As a result, since $\gamma = 0$ (as determined previously), it is reasonable to accept that the reaction is first order, with respect to compound 2 (2b) ($\beta = 1$). Because the overall order of the reaction is $2(\alpha + \beta + \gamma = 2)$, it is obvious that $\alpha = 1$ and order of triphenylphosphine 1 must be equal to one. This observation was obtained also for reactions between (1, 2c and 3) and (1, 2a and 3). Based on the above results, a simplified proposed reaction mechanism is shown in Figure 12.

The experimental results indicate that the third step (rate constant k_3) is possibly fast. In contrast, it may be assumed that the third step is the rate determining step for the proposed mechanism. In this case, the rate law can be expressed as follows:

$$\text{rate} = k_3[I_1][3]. \tag{3}$$

The steady state assumption can be employed for $[I_1]$, which is generated in the following equation:

$$[I_1] = \frac{k_2[1][2]}{k_{-2} + k_3[3]}.$$

The value of $[I_1]$ can be replaced in Eq. (3) to obtain this equation:

$$\text{rate} = \frac{k_2 k_3[1][2][3]}{k_{-2} + k_3[3]}.$$

Since it was assumed that k_3 is relevant to the rate determining step, it is reasonable to make the following assumption:

$$k_{-2} \gg k_3[3].$$

So the rate of low becomes:

$$\text{rate} = \frac{k_2 k_3[1][2][3]}{k_{-2}}.$$

The final equation indicates that the overall order of the reaction is three, which is not compatible with the experimental overall order of the reaction (=2). In addition, according to this equation, the order of reaction, with respect to acetyl acetone 3, is one, whereas it was actually shown to be equal to zero. For this reason, it appeared that the third step is fast. If we assume that the fourth step (rate constant k_4) is the rate-determining step for the proposed mechanism, in this case, there are two ionic species to consider in the rate determining step, namely phosphonium ion (I_2) and acetyl acetone (Z^-). The phosphonium and acetyl acetone ions, as we see in Figure 12, have full positive and negative charges and form very powerful ion-dipole bonds to the 1, 2-dichloroethane; the high dielectric constant solvent. However, the transition state for the reaction between two ions carries a dispersed charge, which here is divided between the attacking acetyl acetone and the phosphonium ions. Bonding of the solvent (1, 2-dichloroethane) to this dispersed charge would be much weaker than to the concentrated charge of acetyl acetone and phosphonium ions. The solvent thus stabilizes the species ions more than it would the transition state and therefore E_a would be higher, slowing down the reaction. However, in practice, 1, 2-dichloroethane speeds up the reaction (see Table 10) and for this reason, the fourth step, which is independent of the change in the solvent medium, could not be the rate determining step. Furthermore, the rate law of formation of the product (fourth step) for a proposed reaction mechanism, by application of steady state assumption, can be expressed by:

$$\text{rate} = k_4[I_2][Z^-].$$

By application of steady state for $[I_2]$ and $[Z^-]$, and replacement of their values in the above equation, the following equation is obtained:

$$\text{rate} = \frac{k_2 k_3[1][2][3]}{k_{-2} + k_3[3]}. \tag{4}$$

This equation is independent of rate constant for the fourth step (k_4) and shows why the fourth step would not be affected by a change in the solvent medium. In addition, it has been suggested earlier that the kinetics of ionic species' phenomena (e.g. the fourth step) are very fast [19–21]. If the first step (rate constant k_2) were the rate determining step, in this case, two reactants (triphenylphosphine 1 and dialkyl acetylenedicarboxylate 2), as we see in Figure 12, would have no charge and could not form strong ion-dipole bonds to the high dielectric constant solvent; 1, 2-dichloroethane. However, the transition state carries a dispersed charge, which here is divided between the attacking 1 and 2 and hence the bonding of solvent to this dispersed charge is much stronger than the reactants, which lack charge. The solvent thus stabilizes the transition state more than it does the reactants and therefore E_a is reduced, which speeds up the reaction. Our experimental results show that the solvent with higher dielectric constant exerts a powerful effect on the rate of reaction (in fact, the first step has rate constant k_2 in the proposed mechanism), but the opposite occurs with the solvent of a lower dielectric constant (see Table 10). The results of the current work (effects of solvent and concentration of compounds) have provided useful evidence for steps 1 (k_2), 3 (k_3) and 4 (k_4) of the reactions between triphenylphosphine 1, dialkyl acetylenedicarboxylate 2 (2a, 2b or 2c) and acetyl acetone 3. Two steps involving 3 and 4 are not determining, although the discussed effects, taken altogether, are compatible with the first step (k_2) of the proposed mechanism and would allow it to be the rate-determining step. However, a good kinetic description of the experimental result, using a mechanistic scheme based upon the steady state approximation, is frequently taken as evidence of its validity. By application of this, the rate formation of product 4 from the reaction mechanism (Figure 12) is given by:

$$\frac{\text{d}[4]}{\text{d}t} = \frac{\text{d}[\text{ylide}]}{\text{d}t} = \text{rate} = k_4[I_2][Z^-]. \tag{5}$$

We can apply the steady-state approximation to $[I_1]$ and $[I_2]$;

$$\frac{\text{d}[I_1]}{\text{d}t} = k_2[1][2] - k_{-2}[I_1] - k_3[I_1][3],$$

$$\frac{\text{d}[I_2]}{\text{d}t} = k_3[I_1][3] - k_4[I_2][Z^-].$$

To obtain a suitable expression for $[I_2]$ to put into Eq. (5), we can assume that after an initial brief period, the concentration of $[I_1]$ and $[I_2]$ achieves a steady state, with their rates of formation and rates of disappearance just balanced. Therefore, $\frac{\text{d}[I_1]}{\text{d}t}$ and $\frac{\text{d}[I_2]}{\text{d}t}$ are zero and we can obtain expressions for $[I_2]$ and $[I_1]$ as follows:

$$\frac{\text{d}[I_2]}{\text{d}t} = 0, \qquad [I_2] = \frac{k_3[I_1][3]}{k_4[Z^-]}, \tag{6}$$

$$\frac{\text{d}[I_1]}{\text{d}t} = 0, \qquad [I_1] = \frac{k_2[1][2]}{k_{-2} + k_3[3]}. \tag{7}$$

We can now replace $[I_1]$ in Eq. (6) to obtain this equation:

$$[I_2] = \frac{k_2 k_3[1][2][3]}{k_4[Z^-]\,[k_{-2} + k_3[3]]}.$$

The value of $[I_2]$ can be put into Eq. (5) to obtain the rate Eq. (8) for the proposed mechanism:

$$\text{rate} = \frac{k_2 k_3 k_4[1][2][3][Z^-]}{k_4[Z^-]\,[k_{-2} + k_3[3]]},$$

or:

$$\text{rate} = \frac{k_2 k_3[1][2][3]}{[k_{-2} + k_3[3]]}. \tag{8}$$

Since experimental data indicated that steps 3 (k_3) and 4 (k_4) are fast, but step 1 (k_2) is slow, it is therefore reasonable to make the following assumption:

$$k_3[3] \gg k_{-2}.$$

So, the rate equation becomes:

$$\text{rate} = k_2[1][2]. \tag{9}$$

This equation, which was obtained from a mechanistic scheme (shown in Figure 12), by applying the steady-state approximation, is compatible with the results obtained by UV spectrometry. With respect to Eq. (9) that shows the overall rate constant (k_2) (Figure 1), the activation parameters involving $\Delta G^{\#}$, $\Delta S^{\#}$ and $\Delta H^{\#}$ could be now calculated in 1, 2-dichloroethane for the first step (rate determining step (k_2)), as an elementary reaction. The results are reported in Table 11.

Table 11: The activations parameters involving $\Delta G^{\#}$, $\Delta S^{\#}$ and $\Delta H^{\#}$ for the reactions between 1, 2a and 3, 1, 2b and 3 and also 1, 2c and 3 at 15.0 °C in 1, 4-dioxane.

Reactions	$\Delta G^{\#}$ (kJ mol^{-1})	$\Delta H^{\#}$ (kJ mol^{-1})	$\Delta S^{\#}$ (kJ mol^{-1})
1, 2a and 3	80.8	9.7	−0.247
1, 2c and 3	81.6	11.3	−0.244
1, 2b and 3	86.5	19.9	−0.231

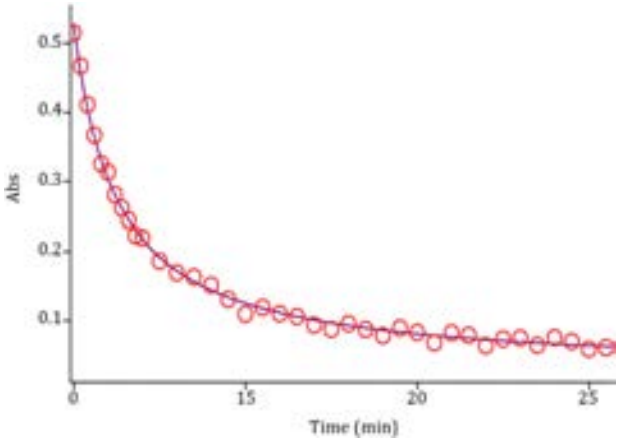

Figure 13: Second order fit curve (solid line) accompanied by the original experimental curve (dotted line) for the reaction between compounds 1, 2c and 3 at 300 nm and 15.0 °C in 1, 4-dioxane.

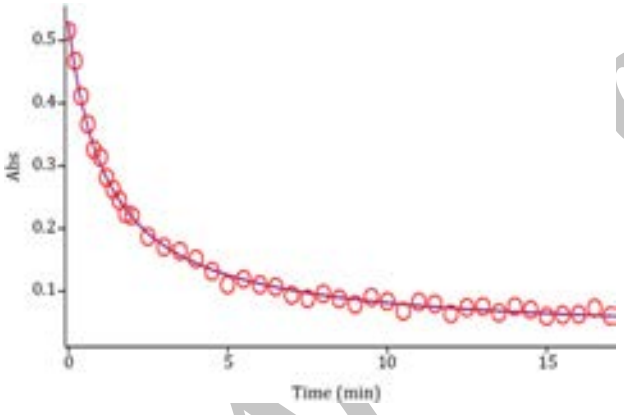

Figure 14: Second order fit curve (solid line) accompanied by the original experimental curve (dotted line) for the reaction between compounds 1, 2a and 3 at 300 nm and 15.0 °C in 1, 4-dioxane.

5.3. Further kinetic investigations (effect of structure of dialkyl acetylenedicarboxylates)

To confirm the above observations, further experiments were performed with diethyl acetylenedicarboxylate 2c and dimethyl acetylenedicarboxylate 2a, respectively, under the same conditions used in the previous experiments. The values of the second-order rate constant (k_2) for the reactions between (1, 2c and 3) and (1, 2a and 3) are reported in Table 10, for all solvents and temperatures investigated. The original experimental absorbance curves (dotted line) accompanied by the second order fit curves (solid line), which exactly fit experimental curves (dotted line) (Figures 13 and 14), confirm previous observations again for both reactions at 15.0 °C and 300 nm.

As can be seen from Table 10, the behavior of diethyl acetylenedicarboxylate 2c and dimethyl acetylenedicarboxylate 2a is the same as for the di-tert-butyl acetylenedicarboxylate 2b (Table 10), with respect to the reaction with triphenylphosphine 1 and acetyl acetone 3. The rate of the former reactions was also accelerated in a higher dielectric constant environment and with higher temperatures; however, these rates under the same condition are approximately 9.48–9.5 times more than for the reaction with di-tert-butyl acetylenedicarboxylate 2b (see Table 10). It seems that both inductive and steric factors for the bulky alkyl groups in 2b tend to reduce the overall reaction rate (see Eq. (9)). In the case of dimetyl acetylenedicarboxylate 2a, the lower steric and inductive effects of the dimethyl groups exert a powerful effect on the rate of reaction.

6. Conclusion

The assignment of the Z- and E-isomers in minor or major forms in both ylides 4a and 4b was undertaken by Atoms In Molecules (AIM) and Natural Population Analysis (NPA) methods and the CHelpG keyword. Quantum mechanical calculation clarified how ylides 4a and 4b exist in solution as a mixture of the two geometrical isomers. This result was in good agreement with the experimental data. In addition, the NMR study on the basis of theoretical calculation was employed for determination of the chemical shifts and coupling constants of the two major Z-4(a,b) and minor E-4(a,b) geometrical isomers, and kinetics investigation of the reactions was undertaken using UV spectrometry. The results can be summarized as follows:

1. The appropriate wavelengths and concentrations were determined to follow the reaction kinetics.
2. The overall reaction order followed second-order kinetics and the reaction orders with respect to triphenylphosphine, dialkyl acetylenedicarboxylate and acetyl acetone were one, one, and zero, respectively.
3. The values of the second-order rate constants of all reactions were calculated automatically, with respect to the standard equation, using the software associated with the Cary-300 UV equipment.
4. The rates of all reactions were accelerated at higher temperatures. Under the same conditions, the activation energy for the reaction with di-tert-butyl acetylenedicarboxylate 2b (24.7 kJ/mol) was higher than that for both reactions, which were followed by the diethyl acetylenedicarboxylate 2c (16.1 kJ/mol) and dimethyl acetylenedicarboxylate 2a (14.5 kJ/mol) in 1, 2-dichloroethane.
5. The rates of all reactions were increased in solvents of higher dielectric constant and this can be related to differences in stabilization by the solvent of the reactants and the activated complex in the transition state.
6. Increased steric bulk in the alkyl groups of the dialkyl acetylenedicarboxylates, accompanied by the correspondingly greater inductive effect, reduced the overall reaction rate.
7. With respect to the experimental data, the first step of the proposed mechanism was recognized as a rate-determining step (k_2) and this was confirmed based upon the steady-state approximation.
8. Also, the third step was identified as a fast step (k_3).
9. The activation parameters involving $\Delta G^{\#}$, $\Delta S^{\#}$ and $\Delta H^{\#}$ were reported for the first step of three reactions.

Acknowledgments

The authors sincerely thank the University of Sistan & Baluchestan for providing financial support for this work.

References

[1] Yavari, I., Anary-abbasinegad, M. and Hossaini, Z. "Reaction between naphthols and dimethyl acetylenedicarboxylate in the presence of phosphites. Synthesis of stable oxa-2λ^5-phosphaphenanthrenes, and benzochromene derivatives", *Org. Biomol. Chem.*, 1, p. 560 (2003).

[2] Yavari, I. and Karimi, E. "Synthesis of stable phosphorus ylides by the reaction of Ph_3P with activated acetylenes in the presence of dimethyl methoxymalonate", *Phosphorus, Sulfur Silicon Relat. Elem.*, 182, p. 595 (2007).

[3] Yavari, I. and Bayat, M. "A new synthesis of highly functionalized 2H-pyran derivatives", *Tetrahedron Lett.*, 59, p. 2001 (2003).

[4] Maghsoodlou, M.T., Habibi-Khorassani, S.M., Nassiri, M., Adhamdoust, S.R. and Salehzadeh, J. "Stable phosphorus ylides and heterocyclic phosphonate esters derivatives synthesised from stereoselective reactions between triphenyl phosphite and activated acetylenic esters", *J. Chem. Res.*, 2, pp. 79–82 (2008).

[5] Hazeri, N., Maghsoodlou, M.T., Habibi, S.M., Nassiri, M. and Afarini, Z. "Study of reaction between triphenylphosphine and activated acetylenic esters in the presence of benzanilide and some of its drivatives", *J. Chem. Res.*, 2, pp. 97–100 (2008).

[6] Maghsoodlou, M.T., Hazeri, N., Habibi-Khorassani, S.M., Mahmoudi Moghaddam, H., Nassiri, M. and Salehzadeh, J. "A facile synthesis of stable phosphorus ylides containing chlorine and sulfur derived from 6-chloro-2benzoxazolethiol and 2-chloro-phenothiazine", *Phosphorus, Sulfur Silicon Relat. Elem.*, pp. 1713–1721 (2009).

[7] Habibi, S.M., Maghsoodlou, M.T., Ebrahimi, A., Kazemian, M.A. and Zakarianezhad, M. "Chemoselective synthesis of stable phosphorus ylides from 6-Azauracil and mechanistic investigation of the reaction by UV spectrophotometry", *Phosphorus, Sulfur Silicon Relat. Elem.*, pp. 2959–2979 (2009).

[8] Habibi, S.M., Ebrahimi, A., Maghsoodlou, M.T., Rostami Charati, F., Kazemian, M.A. and Karimi, P. "A facile synthesis and theoretical study of novel stable heterocyclic phosphorus ylides containing a 2, 4-dimethyl-3-acetyl moiety", *Phosphorus, Sulfur Silicon Relat. Elem.*, pp. 559–566 (2010).

[9] Habibi, S.M., Maghsoodlou, M.T., Ebrahimi, A., Saravani, H., Zakarianezhad, M., Ghahramaninezhad, M., Kazemian, M.A. and Khajehali, Z. "Theoretical study of an efficient synthesis route to and kinetic investigation of stable phosphorus ylides derived from benzamide", *Prog. React. Kinet. Mech.*, pp. 261–288 (2009).

[10] Yavari, I., Nasiri, F. and Djahaniani, H. "Triphenylphosphine catalyzed reaction between 1,3-dicarbonyl compounds and acetylenic esters", *Phosphorus, Sulfur Silicon Relat. Elem.*, 178, pp. 2627–2638 (2003).

[11] Reed, A.E., Weinstock, R.B. and Weinhold, F.J. "Natural population analysis", *J. Chem. Phys.*, 83, pp. 735–742 (1985).

[12] Frisch, M.J., Trucks, G.W. and Schlegel, H.B., et al., *Gaussian 03*, Gaussian, Inc., Pittsburgh, PA Revision A.1 (2003).

[13] Bader, R.F.W., *Atoms in Molecules: A Quantum Theory*, Oxford Univ., New York (1990).

[14] Biegler Konig, F.W., Schonbohm, J. and Bayles, D. "AIM2000- A program to analyze and visualize atoms in molecules", *J. Comput. Chem.*, 22, pp. 545–559 (2001).

[15] Grabowski, S.J. "An estimation of strength of intramolecular hydrogen bonds—ab initio and AIM studies", *J. Mol. Struct.*, 562, pp. 137–143 (2001).

[16] Arnold, W.D. and Oldfield, E. "The chemical nature of hydrogen bonding in proteins via NMR: *J*-coupling, chemical shifts and AIM theory", *J. Am. Chem. Soc.*, 122, pp. 1283–1284 (2000).

[17] Rozas, I., Alkorta, I. and Elguero, J. "Behavior of ylides containing N, O and C atoms as hydrogen bond acceptors", *J. Am. Chem. Soc.*, 122, pp. 11154–11161 (2000).

[18] Schwartz, L.M. and Gelb, R.I. "Alternative method of analyzing first-order kinetic data", *Anal. Chem.*, 50, p. 1592 (1978).

[19] Wolff, M.A., *Chem. Instrum.*, 5, p. 59 (1973).

[20] Treglon, P.A. and Laurence, G.S. "A precision conductance apparatus for studying fast ionic reactions in solution", *J. Sci. Instrum.*, 42, p. 869 (1965).

[21] Okubo, T. and Maeda Kitano, Y. "Inclusion process of ionic detergents with cyclodextrins as studied by the conductance stopped-flow method", *J. Phys. Chem.*, 93, p. 3721 (1989).

Sayyed Mostafa Habibi-Khorassani obtained a Ph.D. degree in Physical Chemistry from the University of Salford, UK. Since 1986, he has been a Faculty member of the Department of Chemistry at the University of Sistan & Baluchestan, Iran, in which he has edited and translated about 12 books during his teaching and research investigations. He has graduated about fifty M.S. and two Ph.D. students and has published about 130 papers in different journals. He is a specialist in Kinetics and Fast Reaction.

Ali Ebrahimi obtained a Ph.D. degree in 2001 and is now Professor of Physical Chemistry at the University of Sistan & Baluchestan, Iran. He has published about 100 papers in different journals and translated various books in different fields of Chemistry. He has graduated about fifty M.S. and one Ph.D. degree students. He is a specialist in Quantum and Computational Chemistry.

Malek Taher Maghsoodlou obtained his Ph.D. degree in Organic Chemistry from Tarbiat Modarres University, Iran, in 1997 and has been a Faculty member of the Department of Chemistry at the University of Sistan & Baluchestan, Iran, since 1984. He has published about 120 papers in different journals and, in addition, has graduated about 60 M.S. and 4 Ph.D. students. He is a specialist in the Synthesis of Heterocyclic Compounds.

Zohreh Khajehali is an M.S. degree student in the Department of Chemistry (Physical Chemistry) at the University of Sistan & Baluchestan, Iran. She has published some papers during her studies in her field of interest.

Mohammad Zakarianezhad is a faculty member in the Department of Chemistry at Payam Noor University, Sirjan Center, Iran. He has published 18 papers during his studies in the field of Physical Chemistry at the University of Sistan & Baluchestan in Iran.